AFRL-PR-WP-TM-2003-2135

LITHIUM POLYMER BATTERY

Dr. Lawrence G. Scanlon, Jr.

Energy Storage and Thermal Sciences Branch (AFRL/PRPS)
Power Division
Propulsion Directorate
Air Force Research Laboratory, Air Force Materiel Command
Wright-Patterson Air Force Base, OH 45433-7251

NOVEMBER 2003

Final Report for 08 December 1994 – 30 December 2002

STINFO FINAL REPORT

PROPULSION DIRECTORATE
AIR FORCE RESEARCH LABORATORY
AIR FORCE MATERIEL COMMAND
WRIGHT-PATTERSON AIR FORCE BASE, OH 45433-7251

NOTICE

USING GOVERNMENT DRAWINGS, SPECIFICATIONS, OR OTHER DATA INCLUDED IN THIS DOCUMENT FOR ANY PURPOSE OTHER THAN GOVERNMENT PROCUREMENT DOES NOT IN ANY WAY OBLIGATE THE US GOVERNMENT. THE FACT THAT THE GOVERNMENT FORMULATED OR SUPPLIED THE DRAWINGS, SPECIFICATIONS, OR OTHER DATA DOES NOT LICENSE THE HOLDER OR ANY OTHER PERSON OR CORPORATION; OR CONVEY ANY RIGHTS OR PERMISSION TO MANUFACTURE, USE, OR SELL ANY PATENTED INVENTION THAT MAY RELATE TO THEM.

THIS REPORT HAS BEEN REVIEWED BY THE OFFICE OF PUBLIC AFFAIRS (ASC/PA) AND IS RELEASABLE TO THE NATIONAL TECHNICAL INFORMATION SERVICE (NTIS). AT NTIS, IT WILL BE AVAILABLE TO THE GENERAL PUBLIC, INCLUDING FOREIGN NATIONS.

THIS TECHNICAL REPORT HAS BEEN REVIEWED AND IS APPROVED FOR PUBLICATION.

LAWRENCE G. SCANLON, JR.
Project Engineer
Energy Storage & Thermal Sciences Branch

JOHN K. ERBACHER
Acting Chief
Energy Storage & Thermal Sciences Branch

CYNTHIA A. OBRINGER
Deputy Chief
Power Division

Do not return copies of this report unless contractual obligations or notice on a specific document requires its return.

REPORT DOCUMENTATION PAGE

Form Approved
OMB No. 0704-0188

The public reporting burden for this collection of information is estimated to average 1 hour per response, including the time for reviewing instructions, searching existing data sources, searching existing data sources, gathering and maintaining the data needed, and completing and reviewing the collection of information. Send comments regarding this burden estimate or any other aspect of this collection of information, including suggestions for reducing this burden, to Department of Defense, Washington Headquarters Services, Directorate for Information Operations and Reports (0704-0188), 1215 Jefferson Davis Highway, Suite 1204, Arlington, VA 22202-4302. Respondents should be aware that notwithstanding any other provision of law, no person shall be subject to any penalty for failing to comply with a collection of information if it does not display a currently valid OMB control number. **PLEASE DO NOT RETURN YOUR FORM TO THE ABOVE ADDRESS.**

1. REPORT DATE *(DD-MM-YY)*	2. REPORT TYPE	3. DATES COVERED *(From - To)*
November 2003	Final	12/08/1994 – 12/30/2002

4. TITLE AND SUBTITLE
LITHIUM POLYMER BATTERY

5a. CONTRACT NUMBER
In-house

5b. GRANT NUMBER

5c. PROGRAM ELEMENT NUMBER
62203F

6. AUTHOR(S)
Dr. Lawrence G. Scanlon, Jr.

5d. PROJECT NUMBER
3145

5e. TASK NUMBER
22

5f. WORK UNIT NUMBER
9D

7. PERFORMING ORGANIZATION NAME(S) AND ADDRESS(ES)

Energy Storage and Thermal Sciences Branch (AFRL/PRPS)
Power Division
Propulsion Directorate
Air Force Research Laboratory, Air Force Materiel Command
Wright-Patterson Air Force Base, OH 45433-7251

8. PERFORMING ORGANIZATION REPORT NUMBER

AFRL-PR-WP-TM-2003-2135

9. SPONSORING/MONITORING AGENCY NAME(S) AND ADDRESS(ES)
Propulsion Directorate
Air Force Research Laboratory
Air Force Materiel Command
Wright-Patterson Air Force Base, OH 45433-7251

10. SPONSORING/MONITORING AGENCY ACRONYM(S)
AFRL/PRPS

11. SPONSORING/MONITORING AGENCY REPORT NUMBER(S)
AFRL-PR-WP-TM-2003-2135

12. DISTRIBUTION/AVAILABILITY STATEMENT
Approved for public release; distribution is unlimited.

13. SUPPLEMENTARY NOTES
Report contains color. One of the authors is a U.S. Government employee; therefore, the U.S. Government is joint owner of the work. If published, the Electrochemical Society may assert copyright. If so, the United States has for itself and others acting on its behalf an unlimited, nonexclusive, irrevocable, paid-up royalty-free worldwide license to use for its purposes.

14. ABSTRACT

This report focuses on the development of a lithium-ion conducting channel as a solid-state electrolyte for rechargeable lithium batteries. Dilithium phthalocyanine (Li_2Pc) has been used in this development since it can undergo molecular self-assembly to form the ionically conducting channel. The essential features of the channel are that it is designed such that the anion matrix of the unsaturated macrocycle forms the channel through which the lithium ion moves, thus making it a single-ion conductor for lithium ions; the ionic transport of lithium depends on the electric field gradient created by the electrodes, thereby minimizing temperature for ionic transport.

15. SUBJECT TERMS
Solid-state electrolyte, lithium-ion conducting channel, lithium battery, ionic conduction

16. SECURITY CLASSIFICATION OF:

a. REPORT	b. ABSTRACT	c. THIS PAGE
Unclassified	Unclassified	Unclassified

17. LIMITATION OF ABSTRACT:
SAR

18. NUMBER OF PAGES
26

19a. NAME OF RESPONSIBLE PERSON (Monitor)
Dr. Lawrence G. Scanlon, Jr.

19b. TELEPHONE NUMBER *(Include Area Code)*
(937) 255-2832

Standard Form 298 (Rev. 8-98)
Prescribed by ANSI Std. Z39-18

i

Table of Contents

iii

List of Figures

List of Tables

1. **INTRODUCTION**

We have been interested in developing a lithium-ion conducting channel for use as a solid-state electrolyte for rechargeable lithium batteries. In this concept, the transference number of lithium is unity, and lithium-ion transport through the electrolyte should primarily depend on the electric field gradient established by the electrodes of the battery, thereby minimizing any temperature dependence for ionic transport. Our initial work in this area has been published in the Proceedings of the International Workshop on Electrochemical Systems, editors A. Landgrebe and R. Klingler, Proceedings Volume 2000-36, page 326, The Electrochemical Society, Inc. 2001. In this paper, the concept of a lithium-ion conducting channel is discussed. Experimental results are based on electrochemical cells composed of a lithium metal anode, Li_2Pc as the solid-state electrolyte, and copper as the working electrode. It is now recognized that increasing the lithium ion concentration in the electrolyte through a reduction process at the copper working electrode contributes greatly to the high specific ionic conductivity of the electrolyte reported in this paper. The increase in lithium ion concentration within the electrolyte was verified by Dr. Rex Gerald at Argonne National Laboratory using solid-state Lithium-7 nuclear magnetic resonance (NMR) for the same cell configuration as described above. His experimental setup allowed him to run both NMR and electrochemical experiments with one specially designed electrochemical cell. Thus, he could do a reduction step at the copper working electrode and then run an NMR experiment immediately thereafter to observe an increase in the lithium ion concentration within the electrolyte at two non-equivalent sites. He also observed that after a lengthy reduction step at the copper working electrode that the NMR signal due to lithium metal completely disappeared.

While the work described above was for an electrochemical half cell, this final report describes a full electrochemical cell composed of a lithium foil metal anode, Li_2Pc with a fluorinated binder as the solid-state electrolyte and a manganese dioxide cathode. This work was submitted for publication to the *Journal of the Electrochemical Society* and thus the final report is in the format of a journal article. The most significant results of this work were the fabrication of full electrochemical cells with stable open circuit voltages and the demonstration, through slow-scan cyclic voltammetry, that lithium ions were transported between the electrodes through the Li_2Pc solid-state electrolyte, as evidenced by the charging and discharging profile for the cyclic voltammograms with a Li_xMnO_2 cathode.

2. COMPOSITE CATHODE WITH Li$_2$Pc

L. G. Scanlon[a], L. R. Lucente[b], W. A. Feld[c], G. Sandí[d], P. B. Balbuena[e], P. R. Alonso[e], and A. Turner[b]

[a]Air Force Research Laboratory, Energy Storage & Thermal Sciences Branch, Wright-Patterson Air Force Base, OH 45433

[b]University of Dayton Research Institute, 300 College Park, Dayton, OH 45469

[c]Department of Chemistry, Wright State University, Dayton, OH 45435

[d]Chemistry Divison, Argonne National Laboratory, 9700 South Cass Ave., Argonne, IL 40439

[e]Department of Chemical Engineering, University of South Carolina, Columbia, SC 29208

Abstract

Computational chemistry calculations performed with Gaussian 98 were used to develop an experimental method that facilitates ionic connection between the solid-state electrolyte dilithium phthalocyanine (Li$_2$Pc) and manganese dioxide (MnO$_2$). The planar configuration of the phthalocyanine ring and the fact that the lithium ions are very close to the ring may sterically hinder effective ionic coupling between Li$_2$Pc and any potential cathode. This same argument has been used for understanding the insertion and removal of magnesium from water solutions of deuteroporphyrins. Calculated results show that lithium ions are drawn closer to the phthalocyanine ring upon formation of (Li$_2$Pc)$_2$ via molecular self-assembly when compared to the single-molecule Li$_2$Pc. However, extension of lithium ions above the planar phthalocyanine ring in (Li$_2$Pc)$_2$ can be enhanced through formation of a complex at the axial position above lithium. Calculations show that coroannulene at the axial position above lithium forms an asymmetric structure with (Li$_2$Pc)$_2$ and does extend lithium further above the ring. To test the theoretical results, an electrically conducting carbon with a curved lattice was used in the fabrication of an all solid-state electrochemical cell with a lithium metal foil anode, Li$_2$Pc electrolyte, and a MnO$_2$ cathode. Slow-scan-rate cyclic voltammograms of a Li$_x$MnO$_2$ cathode demonstrate the charging and discharging of cells.

Introduction

Li$_2$Pc has been under development in our lab as a solid-state lithium-ion conducting channel.[1] Attempts at preparing galvanic cells with lithium metal anodes, Li$_2$Pc and transition metal cathodes have not been successful. It is possible that the failure of these cells is due to poor ionic connectivity between the solid-state electrolyte and the solid-state cathode. The planar configuration of the phthalocyanine ring may sterically hinder effective ionic coupling between Li$_2$Pc and any potential cathode. This same type of argument was previously used to account for the difficulty associated with insertion and removal of magnesium from deuteroporphyrins.[2,3] In this paper, computational chemistry calculations performed with Gaussian 98 were used to develop an experimental method that facilitates ionic connection between the solid-state electrolyte (Li$_2$Pc) and MnO$_2$.[4] Ab initio and classical molecular dynamics results are used to describe lithium-ion channel formation via molecular self-assembly and the importance of an asymmetric structure for facilitating lithium-ion transfer between the electrolyte and cathode. Experimental results showing charging and discharging in a lithium/MnO$_2$ cell are also presented.

Experimental/Computational Methods

Li$_2$Pc was purchased from Aldrich and recrystallized from an acetone/toluene mixture.[5] The resulting microcrystalline material was dried at 130°C under a vacuum of 90 millitorr for 18 hours. MnO$_2$ was provided by Chemetals, Inc. (CMD gamma-MnO$_2$). KYNAR vinylidene fluoride resin (KYNAR FLEX 2801) was purchased from Elf Atochem North America, Inc. Polyvinylidene Fluoride (PVDF) binder and acetylene black were purchased from Aldrich. Battery-grade lithium foil was purchased from FMC Corporation, North Carolina. The solid-state electrolyte was prepared by mixing Li$_2$Pc and KYNAR FLEX 2801 (8 percent by wt. binder) with a Crescent WIG-L-BUG. The composite cathode was prepared by mixing MnO$_2$ (10.9 percent by wt.), carbon (15.1 percent by wt.), Li$_2$Pc (66.6 percent by wt.), and binder (7.4 percent by wt.) in a Crescent WIG-L-BUG. All electrochemical cells were prepared in a dry room where the moisture content is less than 1 percent. The mixed-composite cathode material was placed within a rubber O-ring on battery-grade aluminum foil and sandwiched between two copper plates. The cathode material was then pressed into a pellet at high pressure (3,000 psi) using a Carver press. The area of the pressed cathode was 1.6 cm^2. Once the composite cathode was pressed, a new O-ring was positioned around the cathode pellet and the mixed electrolyte was placed on top of the cathode. Pressure was then applied to form a new pellet, which was a combination of electrolyte and cathode. Typical electrolyte thicknesses range in value from 400 to 700 µm. To complete formation of the galvanic cell, lithium foil approximately 150 µm thick and with an area of 0.785 cm^2 was placed on top of the pressed electrolyte/cathode pellet. The entire galvanic cell fabricated in this configuration was hermetically sealed and under pressure.

A Tenney environmental chamber was used to maintain the operating temperature of the cell. Thermocouples inside the chamber and positioned near the cell monitored the temperature. The temperature range was varied from +21°C to +75°C. Alternating current (AC) impedance and cyclic voltammetry measurements were performed using EG&G electrochemical instruments consisting of the EG&G potentiostat/galvanostat model 273A and EG&G lock-in amplifier model 5210. The amplitude of the AC signal was 5 mV over the frequency range between 100

kHz and 0.1 Hz. Both the spectrometer and the environmental chamber were located in our dry room. Infrared spectra were obtained via a Mattson Genesis II Fourier Transform Infrared (FTIR).

Gaussian 98 was used to perform geometry optimizations and frequency calculations for Li_2Pc and $(Li_2Pc)_2$.[4] Density functional theory was used for these optimizations. The specific method of calculation was Becke-style 3-Parameter Density Functional Theory (B3LYP) with a 3-21G and 6-31G(d) basis sets. Frequency calculations were performed using the 3-21G basis set.

Classical molecular dynamics (MD) simulations were performed in the microcanonical ensemble for a system in orthorhombic crystal structure (tP8, a=19.5 Å, b=19.5 Å, and c=13.2 Å) containing eight molecules in the unit cell, which is periodically repeated in the three spatial directions. The force field contains intramolecular (bond, angle, and dihedral) terms, and intermolecular interactions represented by the 12-6 Lennard Jones potential and Coulombic forces corrected by the Ewald sum to account for long-range interactions.[6] The force field has the basic functional form as the Universal Force Field,[7] with parameters calculated according to the equations in the original reference. Charge distribution was obtained from density functional theory calculations for a single Li_2Pc molecule. Once MD simulations were equilibrated, production runs of 500 ps were carried out to obtain structural properties such as radial distribution functions and structure factors. Further, as discussed in the Results and Discussion section, a small portion of the equilibrated system in the unit cell was extracted to calculate the electrostatic potential based on a single-point calculation using density functional theory. All MD simulations were performed with the DL_POLY program.[8]

At Argonne National Laboratory, carbonaceous materials with enhanced lithium capacity have been derived from ethylene or propylene upon incorporation in the vapor phase in the channels of sepiolite, taking advantage of the Brønsted acidity in the channels to polymerize olefins.[9] Sepiolite is a phyllosilicate clay insofar as it contains a continuous two-dimensional tetrahedral silicate sheet. However, it differs from other clays in that it lacks a continuous octahedral sheet structure. Instead, its structure can be considered to contain ribbons of 2:1 phyllosilicate structure, with each ribbon linked to the next by inversion of SiO_4 tetrahedra along a set of Si-O-Si bonds. In this framework, rectangular channels run parallel to the X-axis between opposing 2:1 ribbons, which results in a fibrous morphology with channels running parallel to the fiber length. Channels are 3.7 x 10.6 Å in sepiolite (they are 3.7 x 6.4 Å in palygorskite). Individual fibers generally range from about 100 Å to 4 to 5 µm in length, 100 to 300 Å width, and 50 to 100 Å thickness. Inside the channels are protons, coordinated water, a small number of exchangeable cations, and zeolitic water. Carbon fibers (1 to 1.5 µm long) are obtained whose orientation and shape resemble that of the original clay. The selected-area electron diffraction (SAED) pattern of the carbon fibers shows diffuse rings typical of amorphous carbon; no diffraction spots were observed.

Carbon Synthesis

Ethylene and propylene (AGA, 99.95 percent) were loaded in the sepiolite samples and pyrolyzed in the gas phase in one step using a three-zone furnace. Quartz boats containing sepiolite were placed within a quartz tube. The tube was initially flushed with nitrogen for about 3 hours. The gas was then switched to propylene or ethylene, and the gas flow was kept at about 5 cm^3/min. The temperature of the oven was gradually increased from room temperature (about 5°C/min) to 700°C. The oven was then held at that target temperature for 4 hours. The clay from the loaded/pyrolyzed sepiolite sample was removed using hydrogen fluoride (HF), previously cooled at 0°C to passivate the exothermic reaction. The resulting slurry was stirred for about 1 hour. It was then rinsed to neutral pH and refluxed with concentrated HCl for 2 hours. The sample was washed with distilled water until the pH was > 5 to ensure that there was no acid left. The resultant carbon was oven dried over night at 120°C.

Results and Discussion

Molecular Self-Assembly

To develop the idea of a lithium-ion conducting channel via molecular self-assembly as a solid-state electrolyte for lithium ions, the molecular structures for Li_2Pc and $(Li_2Pc)_2$ were calculated using density functional theory. Figure 1 shows the top and side views of the calculated structure for Li_2Pc using the 3-21G basis set. The separation between lithium ions is 1.94 Å. The calculated structure using the 6-31G(d) basis set shows that the lithium ions are separated by 1.99 Å.
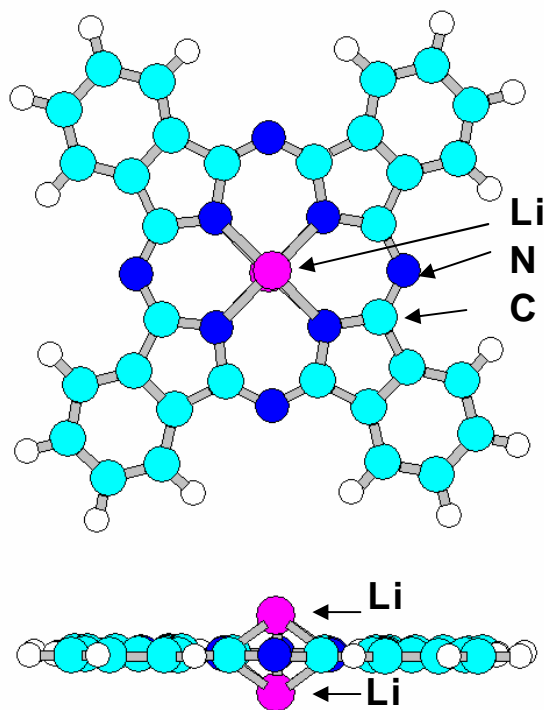

Figure 1 Optimized geometry for Li_2Pc; (a) top and (b) side views using B3LYP/3-21G for the ab initio calculation

Figures 2 and 3 show the calculated structures for $(Li_2Pc)_2$ using the 3-21G basis set as staggered and shifted sandwich complexes, respectively, which result from the electrostatic attraction between lithium ions and nitrogen atoms in adjacent phthalocyanine rings. It is the magnitude of this electrostatic attraction that is important for the molecular self-assembly process. Phthalocyanine ring separation for the staggered structure is 3.38 Å, and where one ring relative to the other is rotated by an angle of 19° (intrastack staggering angle). The corresponding staggered structure optimized with the 6-31G(d) basis set (not shown) has a phthalocyanine ring separation of 3.72 Å and an intrastack staggering angle of 28°.
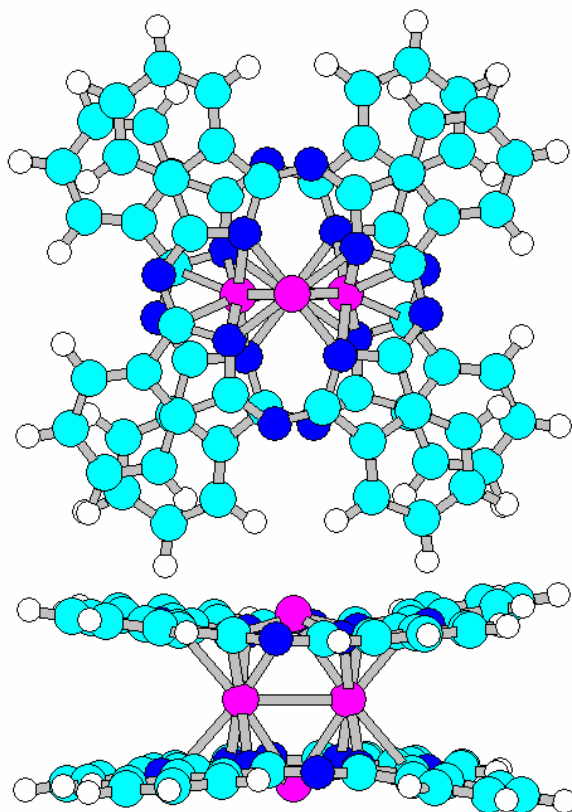

Figure 2 Optimized geometry for the staggered structure of $(Li_2Pc)_2$; (a) top and (b) side views using B3LYP/3-21G for the ab initio calculation

The shifted structure shown in Figure 3 has a phthalocyanine ring separation of 3.65 Å. The corresponding structure using the 6-31G(d) basis set (not shown) for optimization has a ring separation of 3.77 Å. Marks has reported that staggering angles appear to be a function of separation or spacing of the phthalocyanine rings,[10] i.e., phthalocyanine rings are expected to be staggered if ring separation is less than 3.5 Å but, on the other hand, if ring separation is greater than 3.5 Å, then a staggering angle near zero is expected. This general trend may not apply to our molecular system since the adjacent phthalocyanine rings are coupled through two points of contact, whereas in the chemical systems investigated by Marks, the pthalocyanine rings are

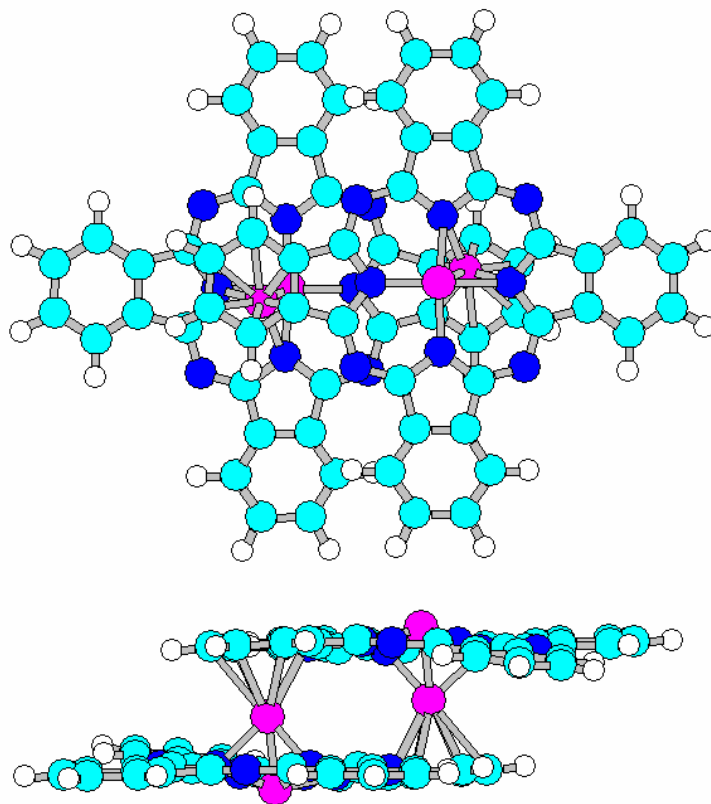connected through a single oxygen atom acting as a bridge between the phthalocyanine rings.

Figure 3 Optimized geometry for the shifted structure of $(Li_2Pc)_2$; (a) top and (b) side views using B3LYP/3-21G for the ab initio calculation

Table 1 shows the computed electronic energies for Li_2Pc and the sandwich complexes $(Li_2Pc)_2$. The binding energies shown in Table 1 are the result of the electrostatic attraction between adjacent phthalocyanine molecules due to the partial positive and negative charges on the lithium and nitrogen atoms, respectively. There is a net stabilization as the result of this interaction, and it is this attraction which accounts for the molecular self-assembly process necessary for channel formation. Figure 4 shows the infrared spectrum of recrystallized Li_2Pc. Prominent bands are the C-C stretch at 1604 cm^{-1}, and the C-H in-plane and out-of-plane bending at 1115 and 729 cm^{-1}, respectively.

Table 1. Computed Energies (Hartrees) and Binding Energies (kcal/mol) for Li$_2$Pc and (Li$_2$Pc)$_2$

Method/Basis Set	Electronic Energy	Electronic Energy	Binding Energy
	Li$_2$Pc	(Li$_2$Pc)$_2$	
RB3LYP/3-21G	-1673.06456	-3346.20214*	45.8
RB3LYP/3-21G		-3346.19101**	38.8
RB3LYP/6-31G(d)	-1682.35746	-3364.74344*	17.9
RB3LYP/6-31G(d)		-3364.74572**	19.3

* Staggered Configuration
** Shifted Configuration

There is a very strong band at 1056 cm^{-1} and a band that appears as a shoulder at 1089 cm^{-1}. Marks has investigated cofacially joined metal phthalocyanine polymers bridged by oxygen (M(phthalocyaninato)O)$_n$, where M is Si, Ge, and Sn.[11] The infrared spectra of these polymeric complexes show a very strong C-N stretching band at 1080, 1087, and 1089 cm^{-1}, respectively. Table 2 shows experimental infrared data for Li$_2$Pc and the calculated frequencies for the shifted and staggered structures using the 3-21G basis set. The calculated results suggest that the very strong band observed experimentally at 1056 cm^{-1} is associated with the C-N stretching vibration. The computed infrared spectrum associated with the shifted structure predicts a very intense C-N stretching vibration at 1026 cm^{-1}. For the staggered structure, this band appears at 1007 cm-^{1}. These results suggest that the shifted structure might be the prominent phase associated with recrystallized Li$_2$Pc.
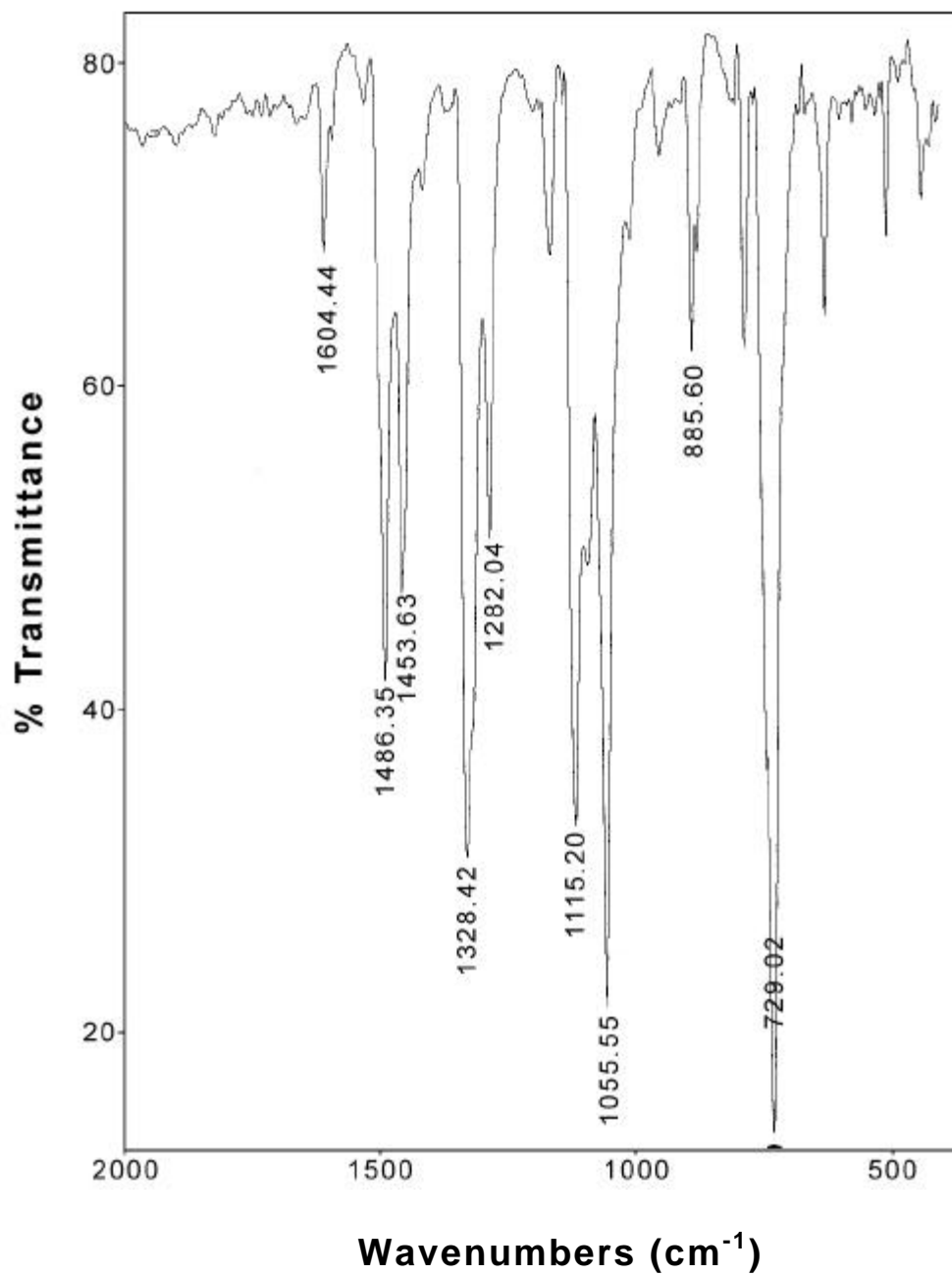
Figure 4 Infrared spectrum of recrystallized Li₂Pc

Table 2. Experimental and Calculated Frequencies for Li$_2$Pc (Wavenumbers)

Experimental	Calculated	
	(Li$_2$Pc)$_2$*	(Li$_2$Pc)$_2$**
729	766 (0.95)***	773 (0.94)
1056	1007 (0.95)	1026 (0.97)
1115	1148 (0.97)	1144 (0.97)
1604	1635 (0.98)	1634 (0.98)
3047	3209 (0.95)	3227 (0.94)

* Staggered Configuration
** Shifted Configuration
*** Scale Factor

Molecular dynamics calculations involving various configurations of Li$_2$Pc are currently being carried out to predict X-ray powder patterns for crystalline samples of Li$_2$Pc which are compared with experimental data.[12] Figure 5 shows a top view of a unit cell and its periodic images for Li$_2$Pc. The shifted or staircase configuration shown on the right-hand side of Figure 5 is considered as a possible pathway for ionic conduction where lithium-lithium separation in the region between the phthalocyanine rings varies from 5.84 to 6.88 Å. It is interesting to note that ab initio calculations for the shifted structure using the 6-31G(d) basis set predicts a separation of 5.89 Å, whereas for the staggered structure, a separation of 2.99 Å is predicted. For ab initio calculations using the 3-21G basis set, these same values are 5.90 and 2.75 Å, respectively.
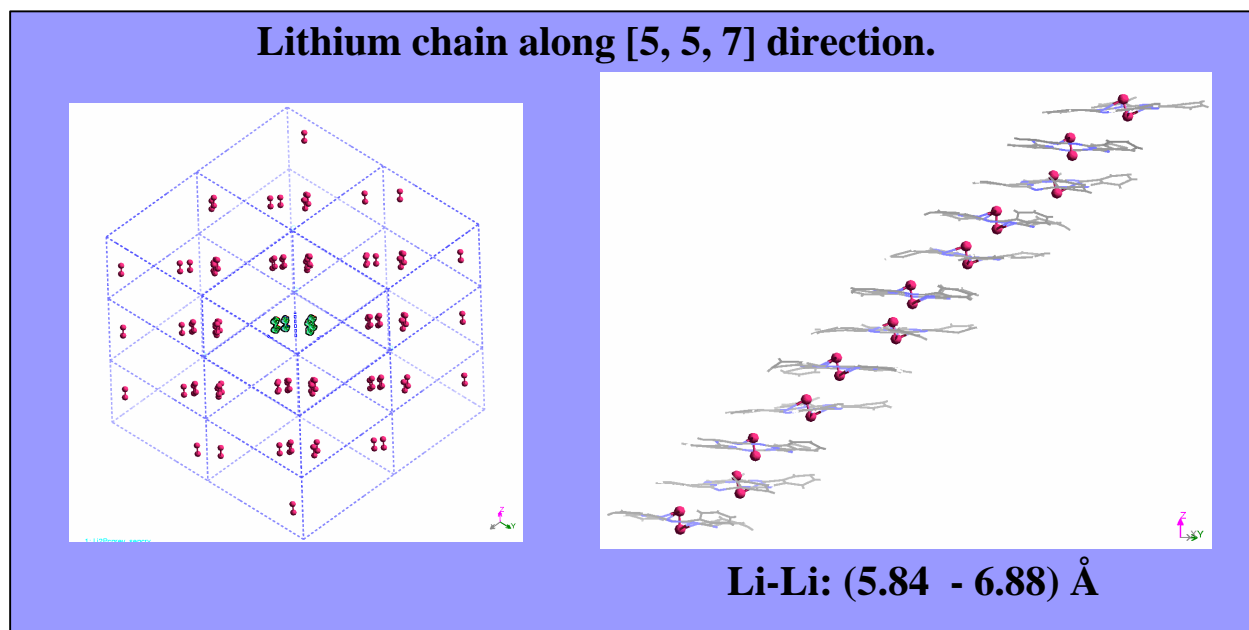

Figure 5 Molecular dynamics calculations illustrating a top view of the unit cell containing eight Li$_2$Pc molecules, and its periodic images, and a possible ionic pathway for lithium-ions

Electrostatic potential contours obtained from an instantaneous molecular dynamics configuration after equilibrations are shown in Figures 6a and 6b. Figure 6a shows the side view of the calculated contours for the molecule in the middle of the three molecules shown. Figure 6b shows the electrostatic potential contours as viewed from the top of the molecular system. The negative region where the lithium ion would travel is clearly defined and shows that the magnitude of this potential is sufficient to show overlap between adjacent phthalocyanine rings even though they have a shifted type of configuration. The molecular dynamics and ab initio calculations suggest that lithium-ion channel formation is possible through a molecular self-assembly process.
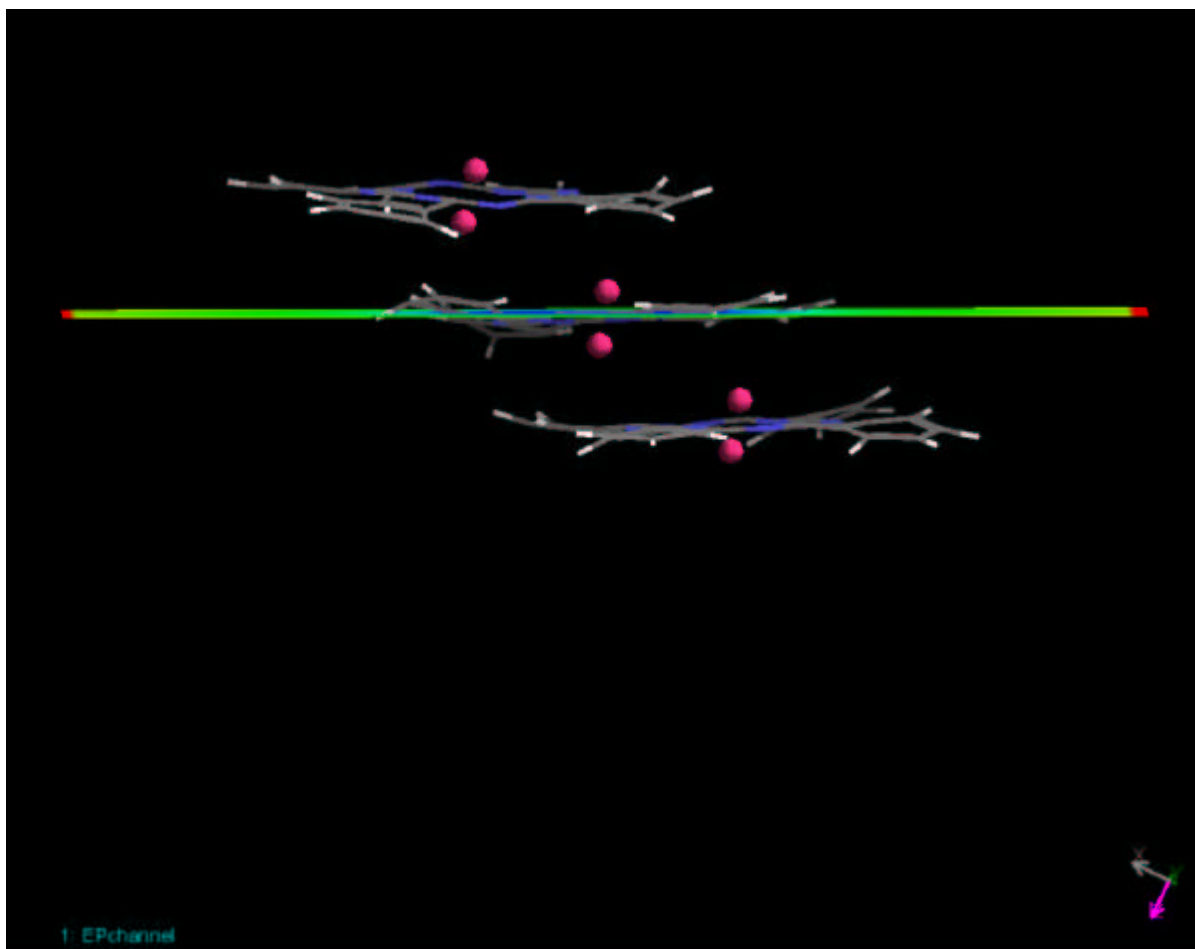

Figure 6a Calculated electrostatic potential contours obtained from molecular dynamics configurations; (a) side view, calculated contours are for the molecule in the middle
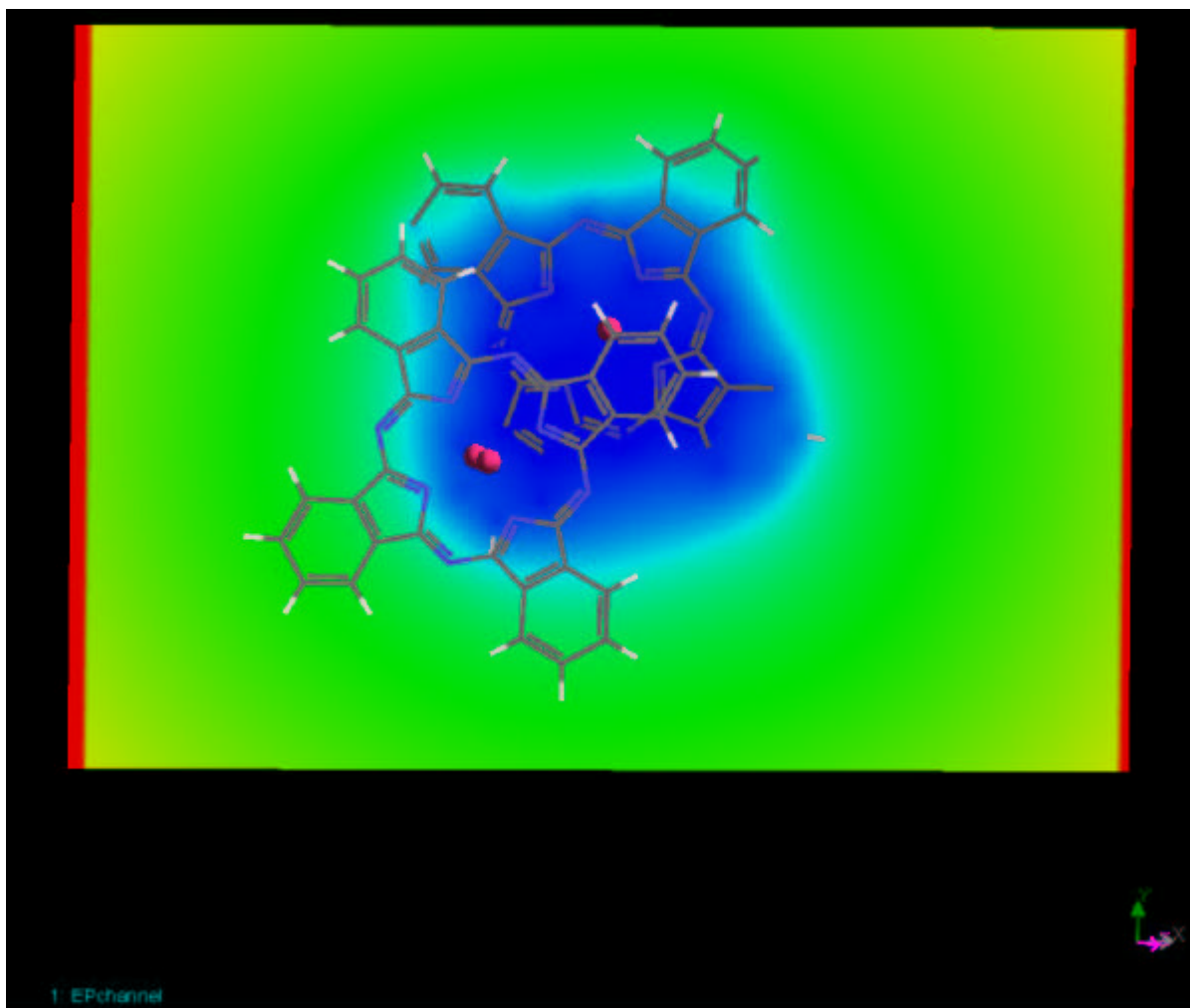
Figure 6b Calculated electrostatic potential contours obtained from molecular dynamics configurations; (b) electrostatic potential contours as viewed from the top of the molecular system

Asymmetric Structure

As discussed above, poor ionic connectivity of the solid-state electrolyte with the cathode could be attributed to the planar configuration of the phthalocyanine ring sterically hindering effective ionic coupling between Li_2Pc and any potential cathode. This coupled with the fact that lithium ions are drawn closer to the phthalocyanine ring upon sandwich complex formation via molecular self-assembly further complicates the ionic coupling issue. For example, in the single-molecule Li_2Pc, the lithium ions are about 1 Å above the plane of the molecule. However, for the shifted sandwich structure $(Li_2Pc)_2$ (optimized using RB3LYP/6-31G(d)) the lithium ions are approximately 0.69 Å above the plane of the molecule. For the corresponding staggered structure using the same method of calculation and basis set for optimization, the extension of the lithium ions above/below the phthalocyanine ring is approximately 0.45 Å. Plane has investigated the kinetics of acid displacement of the magnesium ion from porphyrin.[2] He found that pyridine can have a catalytic effect, and when water is present with pyridine in the activated complex, this too results in an enhanced catalytic effect. In the catalytic process, he thought

displacement of the magnesium ion out of the porphyrin plane to be important. This could occur through formation of a new coordination sphere about magnesium. To illustrate this idea, Figure 7 shows the optimized structure of a MgPc dimer as reported in reference 3 using B3LYP/6-31G(d) for the optimization process.
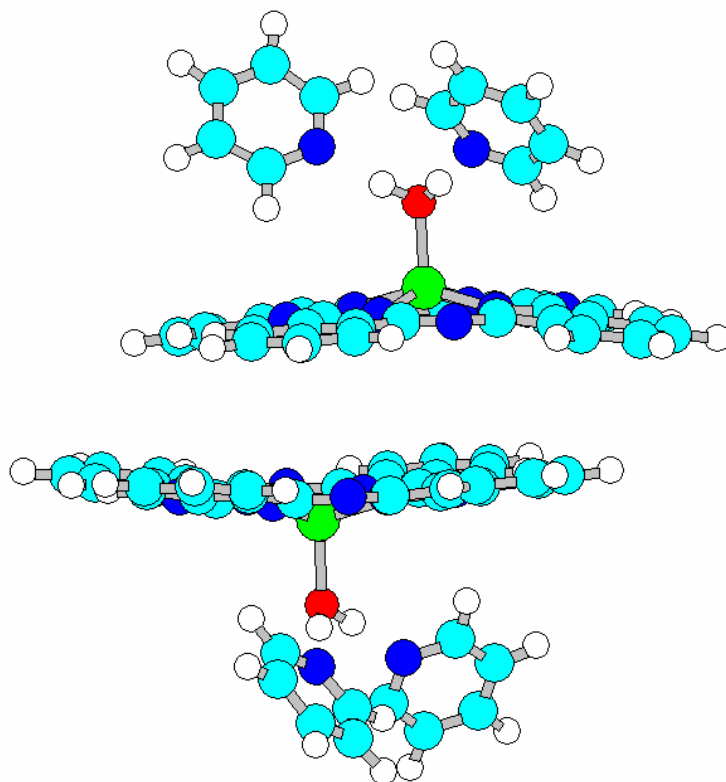

Figure 7 Optimized structure for the MgPc dimer (MgPc-H_2O-$2C_5H_5N$)$_2$ using B3LYP/6-31G(d) for the ab initio calculation

X-ray structural analysis shows the dimer to consist of two asymmetric units in which magnesium of the MgPc unit is bonded to a water molecule and the hydrogen atoms in turn are each bonded to a pyridine molecule through hydrogen bonding. It was suggested by Templeton[3] that a structure like this may explain the catalytic effect of pyridine as reported by Plane[2]. X-ray structural results show that the magnesium ion is displaced 0.496 Å above the plane of the inner nitrogen atoms. The calculated displacement of the magnesium ion from the plane formed by the inner nitrogen atoms is 0.528 Å. In view of the apparent difficultly in making a good ionic connection between Li_2Pc and MnO_2, it was decided to investigate through computational chemistry the effect of a curved carbon lattice, such as corannulene, on the magnitude of the displacement of the lithium ion above the phthalocyanine plane for the shifted structure. This is shown in Figure 8. The calculated displacement of the lithium ion above the phthalocyanine plane for this structure is 1.01 Å. To test the theoretical results, an electrically conducting carbon with a curved lattice was used in the fabrication of an all solid-state electrochemical cell with a lithium metal foil anode, Li_2Pc electrolyte, and a MnO_2 cathode.
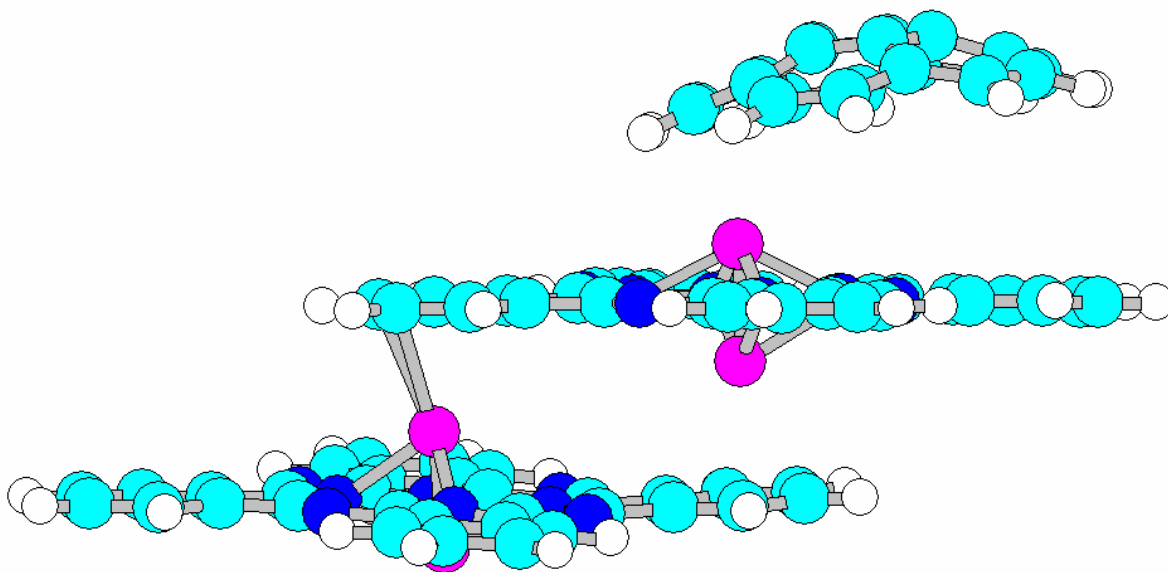
13

Figure 8 Optimized structure for $(Li_2Pc)_2$-corannulene using B3LYP/6-31G(d) for the ab initio calculation

A slow-scan cyclic voltammogram of this cell is shown in Figure 9. Because the construction of this cell is based on pressed pellets for the electrolyte and cathode, there are inherent high impedances within the cell, and the cell had to be operated at 75°C. Total ohmic resistances of the cell before and after the slow-scan cyclic voltammogram are 6.0 and 3.8 kO, respectively.

Figure 10 shows another slow-scan cyclic voltammogram of the same cell 5 days later after being maintained at 75°C. The total ohmic resistance of the cell after the slow-scan cyclic voltammogram was 5.5 kO with an open circuit voltage of 2.70 volts.
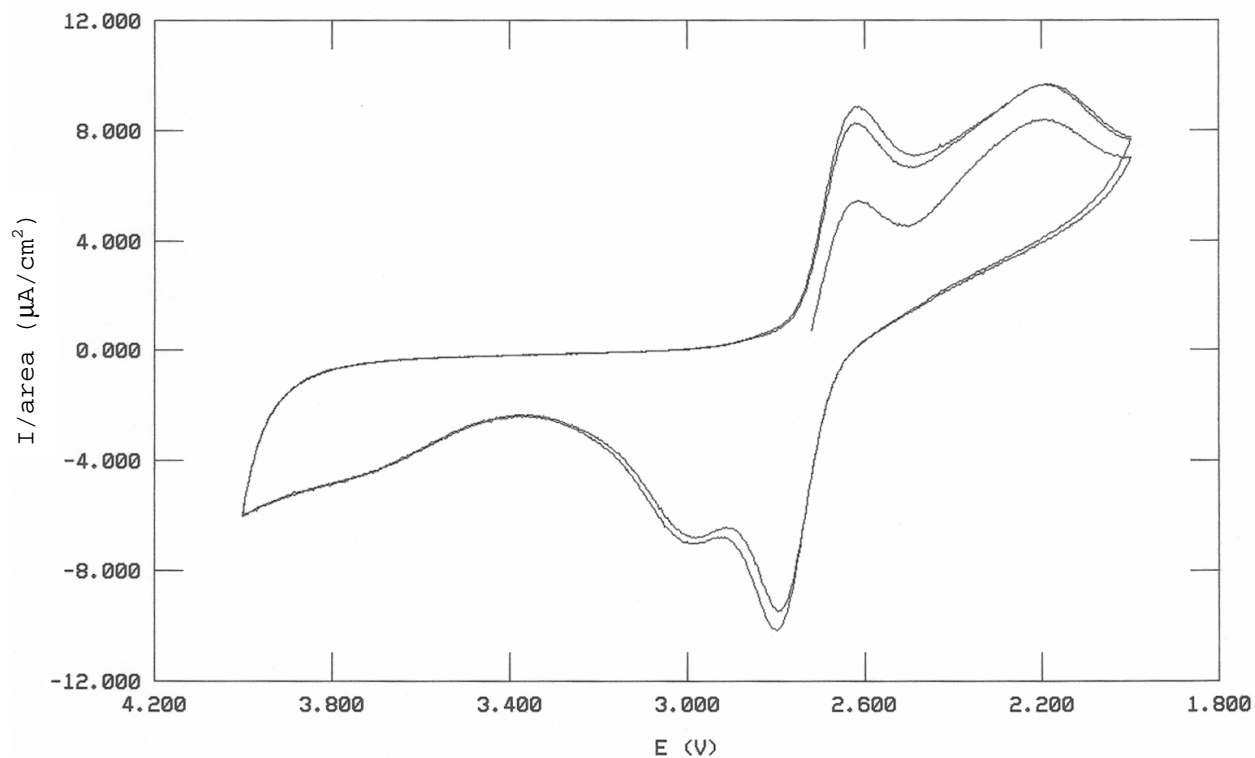
Figure 9 Slow-scan cyclic voltammogram (scan rate 280 µV/s) at 75°C of a Li/Li$_2$Pc/MnO$_2$ cell with carbon with a curved structure in the composite cathode
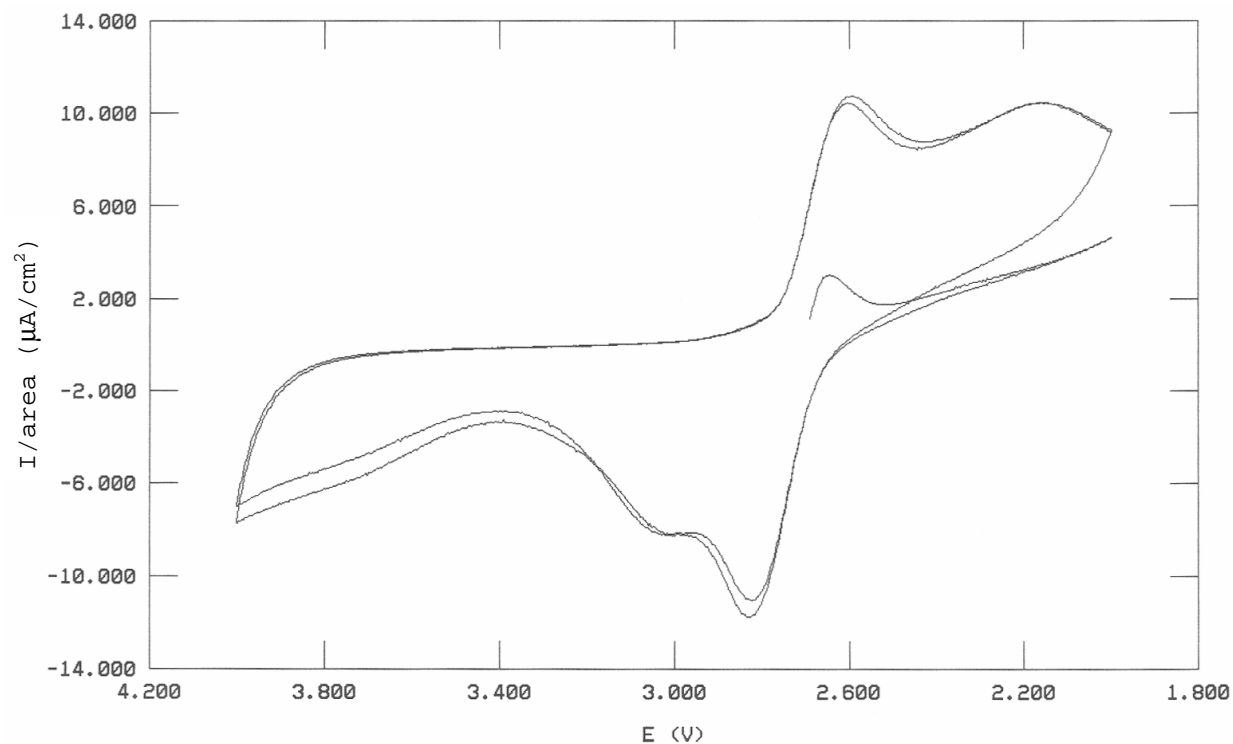

Figure 10 Slow-scan cyclic voltammogram (scan rate 280 µV/s) at 75°C of same cell shown in Figure 9 maintained at 75°C but after 126 hours from previous test

These tests were repeated with other cells using acetylene black as the carbon additive to the composite cathode, and very similar results were attained, as shown in Figure 11. Calculations show that when a planar molecule, such as toluene, is substituted for corannulene in the axial position, lithium is extended 1.06 Å above the phthalocyanine plane.
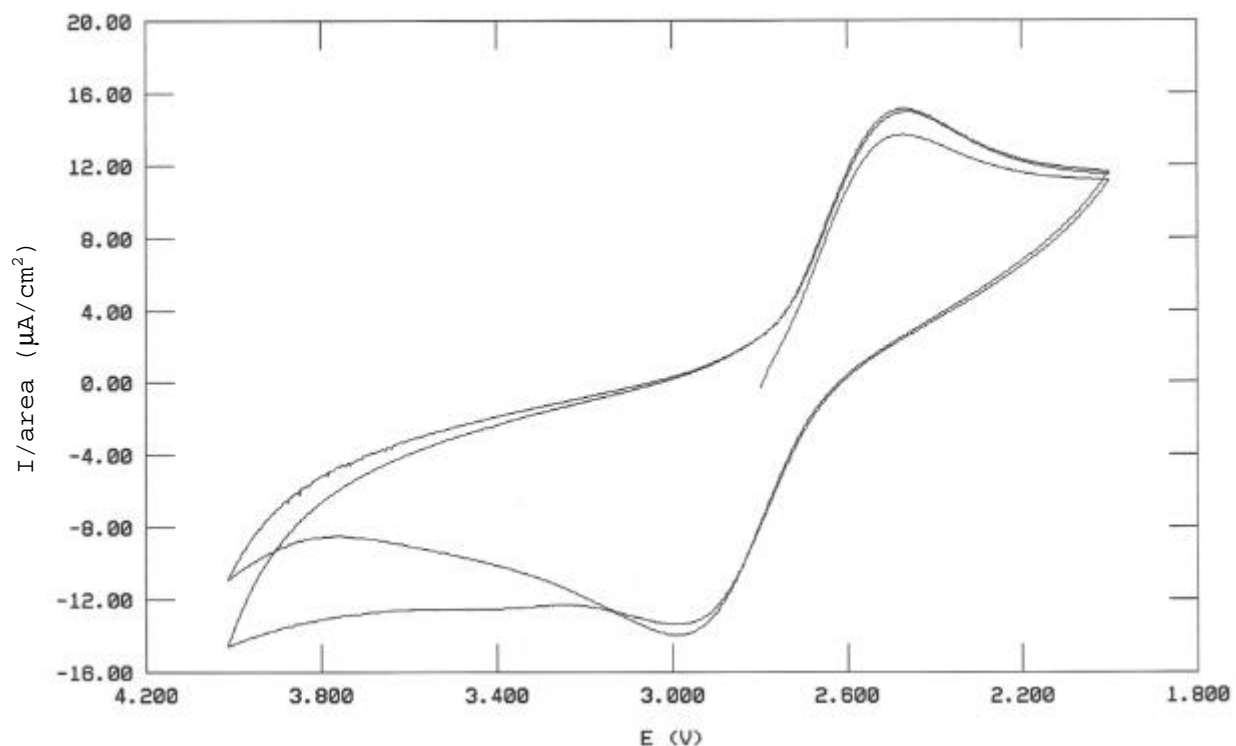

Figure 11 Slow-scan cyclic voltammogram (scan rate 280 µV/s) at 75°C of a Li/Li$_2$Pc/MnO$_2$ cell with acetylene black in the composite cathode

Experimental results show the charging and discharging of the MnO$_2$ cathode with the solid-state electrolyte Li$_2$Pc. Effective ionic coupling of the solid-state electrolyte with the cathode may have been facilitated through coordination of the curved carbon lattice or acetylene black with lithium in Li$_2$Pc.

References

1. L. G. Scanlon, L. R. Lucente, W. A. Feld, G. Sandi, D. J. Campo, A. E. Turner, C. S. Johnson, and R. A. Marsh, "Interfaces, Phenomena, and Nanostructures in Lithium Batteries," A. R. Landgrebe and R. J. Klingler, Editors, PV 2000-36, p. 326, <u>The Electrochemical Society Proceedings Series, Pennington</u>, NJ (2001).

2. R. Snellgrove and R. A. Plane, *J. Am. Chem. Soc*., **90**, 3,185 (1968).

3. M. S. Fischer, D. H. Templeton, A. Zalkin, and M. Calvin, *J. Am. Chem. Soc*., **93**, 2,622 (1971).

4. M. J. Frisch, G. W. Trucks, H. B. Schlegel, G. E. Scuseria, M. A. Robb, J. R. Cheeseman, V. G. Zakrzewski, J. A. Montgomery Jr., R. E. Stratmann, J. C. Burant, S. Dapprich, J. M. Millam, A. D. Daniels, K. N. Kudin, M. C. Strain, O. Farkas, J. Tomasi, V. Barone, M. Cossi, R. Cammi, B. Mennucci, C. Pomelli, C. Adamo, S. Clifford, J. Ochterski, G. A. Petersson, P. Y. Ayala, Q. Cui, K. Morokuma, D. K. Malick, A. D. Rabuck, K. Raghavachari, J. B. Foresman, J. Cioslowski, J. V. Ortiz, B. B. Stefanov, G. Liu, A. Liashenko, P. Piskorz, I. Komaromi, R. Gomperts, R. L. Martin, D. J. Fox, T. Keith, M. A. Al-Laham, C. Y. Peng, A. Nanayakkara, C. Gonzalez, M. Challacombe, P. M. W. Gill, B. Johnson, W. Chen, M. W. Wong, J. L. Andres, C. Gonzalez, M. Head-Gordon, E. S. Replogle, and J. A. Pople, Gaussian 98, Revision A.11, Gaussian, Inc., Pittsburgh, PA (1998).

5. D. Dolphin, J. R. Sams, and T. B. Tsin, *Inorg. Synth*., **20**, 159 (1980).

6. M. P. Allen and D. J. Tildesley, <u>Computer Simulation of Liquids</u>, Oxford University Press (1986).

7. A. K. Rappe, C. J. Casewit, K. S. Colwell, W.A. Goddard and W. M. Skiff, *J. Am. Chem. Soc*., **114**, 10,024 – 10,035 (1992).

8. T. R. Forester and W. Smith, DL_POLY parallel molecular dynamics simulation package CCLRC, Daresbury Laboratory, Daresbury, Warrington WA 4AD, UK, version 2.13, (2001).

9. G. Sandi, K. A., Carrado, R. E. Winans, C. S. Jonson, and R. Csencsits, *J. Electrochem. Soc*., **146**, 3,644 (1999).

10. E. Ciliberto, K. A. Doris, W. J. Pietro, G. M. Reisner, D. E. Ellis, I. Fragala, F. H. Herbstein, M. A. Ratner, and T. J. Marks, *J. Am. Chem. Soc*., **106**, 7,748 (1984).

11. C. W. Dirk, T. Inabe, K. F. Schoch, and T. J. Marks, <u>J. Am. Chem. Soc</u>., **105**, 1,539 (1983).

12. Y. Zhang, P.R. Alonso, A. Martinez-Limia, L. G. Scanlon, and P. B. Balbuena, to be submitted.